HTML ABSTRACT + LINKS

Raman study of As outgassing and damage induced by ion implantation in Zn-doped GaAs

D. Barba,[a] V. Aimez, J. Beauvais, J. Beerens, and D. Drouin
Département de Génie Électrique et de Génie Informatique, Université de Sherbrooke, Sherbrooke, Quebec J1K 2R1, Canada

M. Chicoine and F. Schiettekatte
Département de Physique, Université de Montréal, Montréal, Quebec H3C 3J7, Canada

(Received 19 April 2004; accepted 7 August 2004)

Room temperature micro-Raman investigations of LO phonon and LO phonon-plasmon coupling is used to study the As outgassing mechanism and the disordering effects induced by ion implantation in Zn-doped GaAs with nominal doping level $p=7\times10^{18}$ cm^{-3}. The relative intensity of these two peaks is measured right after rapid vacuum thermal annealings (RVTA) between 200 and 450 °C, or after ion implantations carried out at energies of 40 keV with P^+, and at 90 and 170 keV with As^+. These intensities provide information regarding the Schottky barrier formation near the sample surface. Namely, the Raman signature of the depletion layer formation resulting from As desorption is clearly observed in samples submitted to RVTA above 300 °C, and the depletion layer depths measured in ion implanted GaAs:Zn are consistent with the damage profiles obtained through Monte Carlo simulations. Ion channeling effects, maximized for a tilt angle set to 45° during implantation, are also investigated. These results show that the Raman spectroscopy is a versatile tool to study the defects induced by postgrowth processes in multilayered heterostructures, with probing range of about 100 nm in GaAs-based materials. © *2004 American Institute of Physics*. [DOI: 10.1063/1.1803615]

I. INTRODUCTION

Raman spectroscopy is a powerful nondestructive technique used to study the variation of crystallinity in III-V semiconductors after rapid thermal annealing,[1,2] recrystallizing processes,[3] ion beam etching,[4] and ion implantation.[5,6] Many Raman scattering measurements performed in *n*- and *p*-type materials have put the emphasis on the longitudinal vibration of the carrier plasma which couples with the LO phonon via the macroscopic electric field to form a phonon-like LO phonon-plasmon coupling (LOPC) mode. Such a mechanism has been studied in *p*-type GaAs as a function of different carbon,[7] silicon,[8] beryllium,[9,10] and zinc[11] doping levels. These previous reports have shown that the relative integrated areas of the LO phonon bands (I_{LO}) and the LOPC bands (I_{LOPC}) can directly be connected to the free carrier concentration located in the Raman probed volume, thus allowing one to estimate the depletion layer depth in the vicinity of the sample surface.

In this paper, we present micro-Raman investigation of $p=7\times10^{18}$ cm^{-3} Zn-doped (100) GaAs substrates after rapid vacuum thermal annealings (RVTA) or after ion implantations. We show that this experimental technique can provide both quantitative and qualitative information regarding the defects induced by these two postgrowth processes. The measurements of the I_{LO}/I_{LOPC} ratio between 200 and 400 cm^{-1} are obtained with the help of the data reported by Irmer *et al.* for heavily doped *p*-type GaAs with low carrier mobility.[11] Our results enable us to study the mechanisms involved in the Schottky barrier formation, and to measure the range of the damage these mechanisms generate near the sample surface. First, the evolution of the depletion layer depth observed in RVTA-processed samples is analyzed in terms of surface reconstruction and desorption effects.[12,13] Second, we investigate unannealed P^+ and As^+ implanted materials with different ion beam energies, where tilt angles were set to 7° and 45°, in order to minimize or to maximize the ion channeling, respectively. These measurements are finally compared to the damage profile calculated using SRIM 2003 Monte Carlo simulations.[14]

II. EXPERIMENTS

The RVTA of unimplanted samples were performed during 60 s at 10 mbar, with annealing temperatures varying between 200 and 400 °C. Ion implantations have been carried out at $T=20$ °C using a Tandetron accelerator. P^+ were implanted with ion beam energies of 40 keV, and As^+ ions were implanted into GaAs:Zn with incident energies of 90 and 170 keV. For each of these implantations, the tilt angles were set at 7° and 45° with a precision of ±2°. To avoid amorphization, which occurs at lower thresholds for this implant temperature,[15] the fluences were restricted to 10^{13} ions/cm^2 and 10^{12} ions/cm^2 for P^+ and As^+, respectively.

One cm^{-1} resolution micro-Raman studies were carried out at room temperature in the $z(xy)\bar{z}$ backscattering geometry, using a LABRAM-800 confocal system equipped with a nitrogen-cooled charge-coupled device detector and a 50× microscope lens. A 514.5 nm Ar laser line focused on a diameter spot of few microns and polarized perpendicular to

[a]Electronic mail: dbarba@physique.usherb.ca

 © 2004 American Institute of Physics

Downloaded 20 Dec 2006 to 132.204.95.70. Redistribution subject to AIP license or copyright, see http://jap.aip.org/jap/copyright.jsp

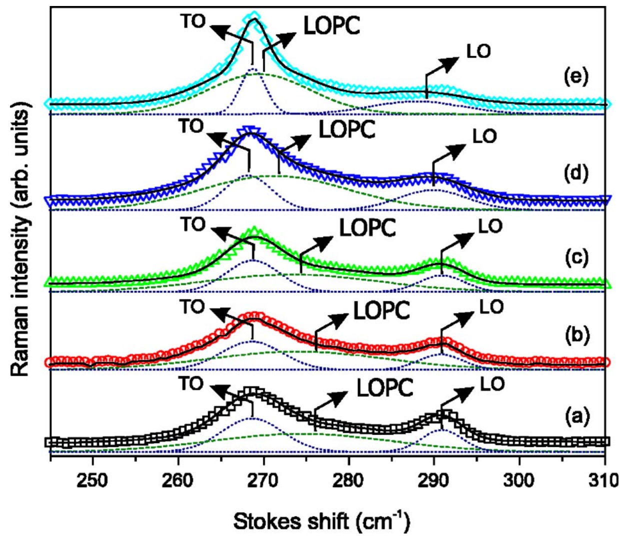

FIG. 1. Raman signature of reference unannealed GaAs:Zn material (a) and vacuum annealed samples during 60 s at $T=250$ °C (b), $T=300$ °C (c), $T=350$ °C (d) and $T=400$ °C (e). The solid lines are the sum of the fitted LOPC (dashed lines), TO phonon, and LO phonon (dots) bands.

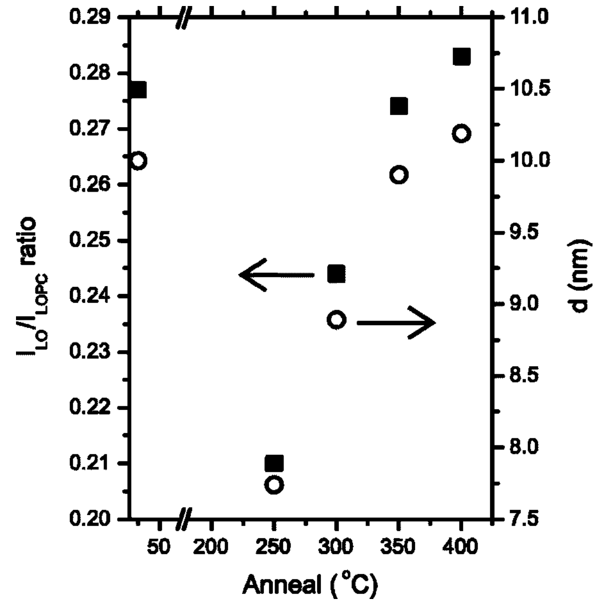

FIG. 2. Relative integrated area of the measured LO phonon and the LOPC mode (■) as a function of annealing temperature, with the corresponding depletion depth (○) calculated from Eq. (1). The data associated with $T=20$ °C designate the unannealed material.

the ⟨100⟩ growth axis of the samples was used for excitation. The laser power was kept at 30 mW to prevent sample heating.

III. RESULTS AND DISCUSSION

A. Raman analysis

Since GaAs belongs to the point group of symmetry T_d, only the LO phonon and the LOPC excitation are dipole allowed in the $z(xy)\bar{z}$ optical configuration. The depths explored by the Raman probe are 60 nm for confocal hole diameter $h=0.5$ mm, and of ≈100 nm for $h=1.0$ mm.[16,17]

Our estimation of the depletion layer depth is based on the Schottky model, assuming that the carrier concentration abruptly rises to the bulk value at a distance d away from the sample surface. According to Ref. 11, this value can be deduced from Raman measurements using the relation

$$d=\frac{\delta}{2}\ln\left(1+\frac{A}{A_0}\right), \tag{1}$$

where δ corresponds to the penetration depth of the laser light with wavelength $\lambda=514.5$ nm, extracted from Ref. 16, A is the measured ratio of the peak integrated intensity I_{LO}/I_{LOPC}, and A_0 refers to the I_{LO}/I_{LOPC} areas ratio calculated in pure GaAs, given in Ref. 11.

B. Vacuum thermal annealed GaAs:Zn

Figure 1 shows the Raman spectra between 240 and 310 cm^{-1} of unimplanted GaAs:Zn, for an unannealed reference sample and for samples annealed at 250, 300, 350, and 400 °C. This set of measurements was obtained by using $h=1$ mm, in order to probe the effects induced by RVTA in the first 100 nm of the materials. The dotted lines denote the fitted forbidden TO and allowed LO phonons bands, observed at 269 and 290 cm^{-1}, respectively. The dashed lines identify the LOPC mode, with energy ranging 270–274 cm^{-1}, and the solid lines refer to the sum of TO phonon, LO phonon, and LOPC bands. The corresponding I_{LO}/I_{LOPC} ratios and depletion depths are estimated using Eq. (1) and reported as a function of the annealing temperature in Fig. 2.

The observation of Raman signal at the TO frequency is associated with disorder effects resulting from Zn doping and so-called forbidden TO-phonon scattering.[18] The measured wave numbers and bandwidths of TO phonon, LO phonon, and LOPC bands are close to those reported by Irmer *et al.*[11] in $p=7.2\times10^{18}$ cm^{-3} GaAs:Zn. The constant energy position of the TO phonon and LO phonon lines indicates low contamination effects resulting from RVTA. On the other hand the LOPC energy softening observed in the samples annealed above 300° C denotes a significant reduction of the carrier mobility in these materials due to the generation of defects within the structure.[11]

The vacuum heating of GaAs leads to surface reconstruction and outgassing effects, which promote the formation of extended defects in the vicinity of the sample surface. Such mechanisms have been studied by means of atomic force microscopy,[12] low-energy electron diffraction measurements, and Auger electron spectroscopy.[13] These previous reports have allowed the authors to describe the surface reconstruction processes induced by thermal annealings performed up to about 350 °C, showing that the As atoms are displaced outward and the Ga atoms inward with respect to the bulk. Above $T=350$ °C, it has been established that both As and Ga atoms desorb from the substrate. However, this process favors the generation of As vacancies in the upper layers of the sample, due to the higher desorption rate of As with respect to Ga between 300 and 600 °C.[19] This scenario is consistent with the data reported in Fig. 2. Indeed, the decrease of the depletion depths from 10 nm in unannealed sample to 7.8 nm in vacuum annealed samples at 250 °C can

Downloaded 20 Dec 2006 to 132.204.95.70. Redistribution subject to AIP license or copyright, see http://jap.aip.org/jap/copyright.jsp

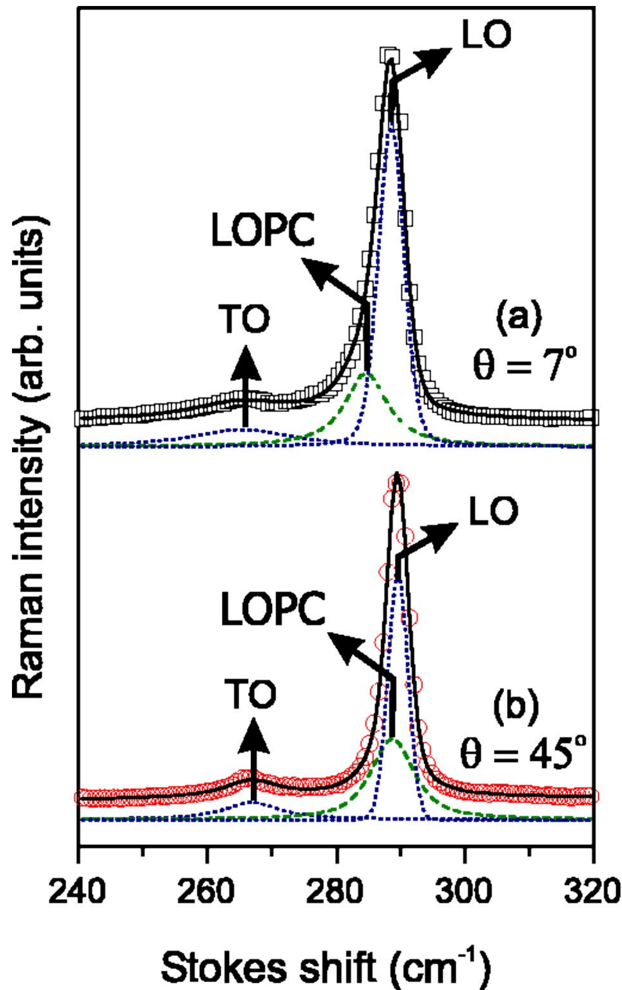

FIG. 3. Room temperature Raman spectra of P^+ implanted GaAs:Zn at 40 keV with tilt angles set to 7° (a) and 45° (b).

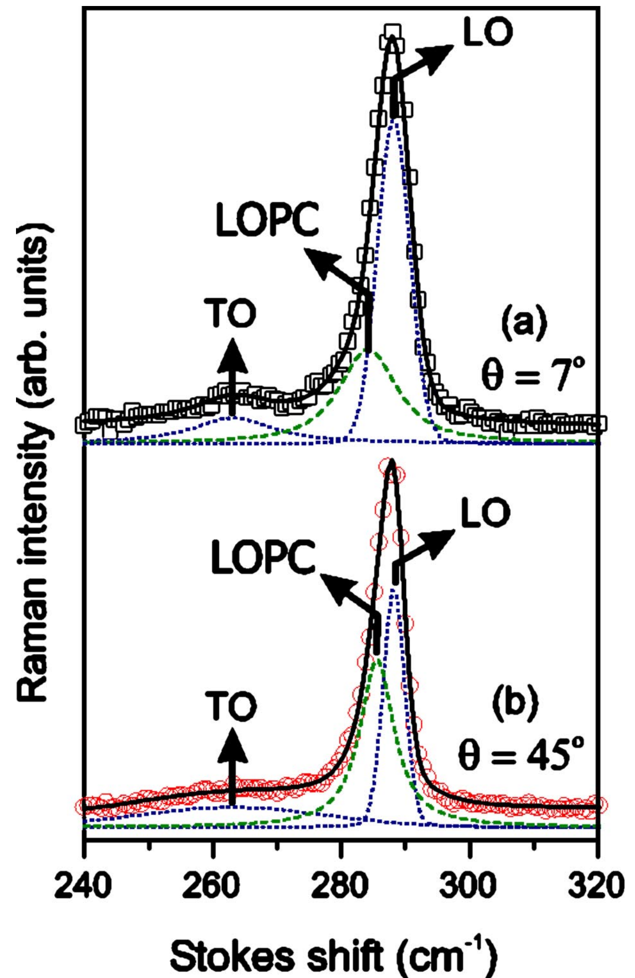

FIG. 4. Room temperature Raman spectra of As^+ implanted GaAs:Zn at 90 keV with tilt angles set to 7° (a) and 45° (b).

be connected to the displacement of the As donors toward the sample surface. On the other hand, the presence of As vacancies excess, resulting from preponderant As desorption during RVTA performed between 300 and 400 °C, agrees with the increase of depletion depths from 7.6 to 10.2 nm in this temperature range (Fig. 2).

C. Ion implanted GaAs:Zn

Figures 3 and 4 illustrate measurements obtained in the 240–320 cm^{-1} spectral range using confocal hole h =0.5 mm and Fig. 5 with h=1.0 mm, so that most of the damage induced by the different ion implantations is located in the Raman probed volume. Figures 3(a) and 3(b) correspond to P^+ implanted materials at 40 keV, with tilt angles equal to 7° (a) and 45° (b), whereas Figs. 4(a) and 4(b) and Figs. 5(a) and 5(b) report on Raman spectra recorded in As^+ implanted material at 90 and 170 keV, respectively. The solid line designates the fitted spectra, which includes the contribution of TO phonon band at 265 cm^{-1}, LO phonon band at 289 cm^{-1}, and LOPC mode around 285 cm^{-1}.

All these Raman spectra exhibit a drastic enhancement of the I_{LO}/I_{TO} ratio by a factor of up to 10 with respect to the unimplanted samples (Fig. 1). Such an increase is associated with impurity-induced Raman scattering,[20] and accompanied by a LO phonon softening of 2 cm^{-1} resulting from ion incorporation within the structure. This energy shift is very close to the value reported by Ashokan *et al.*[5] in P^+ implanted GaAs at 70 keV with fluence of 10^{13} ions/cm^2.

The depletion depths deduced from the measured I_{LO}/I_{LOPC} ratios are reported in the third and fifth columns of Table I with a few nanometers accuracy. These experimental values compare well with the SRIM calculations, giving the average penetration depth R_p of implanted ions in GaAs for corresponding ion beam energy and tilt angle, in fourth and sixth columns of Table I. Although the SRIM simulations do not include ion channeling effects,[14] which increase the longitudinal path of implanted ions within the target,[21] discrepancies of less than 8 nm are observed between measurements and calculations. We note that the depletion layer depths are slightly smaller than expected for the 45° implant angle, thus showing the negligible contribution of channeled ions to the experimental data. These remarks suggest that the formation of a large depletion layer below the sample surface is mainly connected to the range of defects arising from nuclear collisions between host atoms and incident ions, rather than to the spatial distribution of implanted ions. According to electrical conductivity measurements of Zn^+, S^+, and N^+ implanted GaAs,[22] such a feature is due to the trapping of free carriers by atoms displaced from their original site. We conjecture

Downloaded 20 Dec 2006 to 132.204.95.70. Redistribution subject to AIP license or copyright, see http://jap.aip.org/jap/copyright.jsp

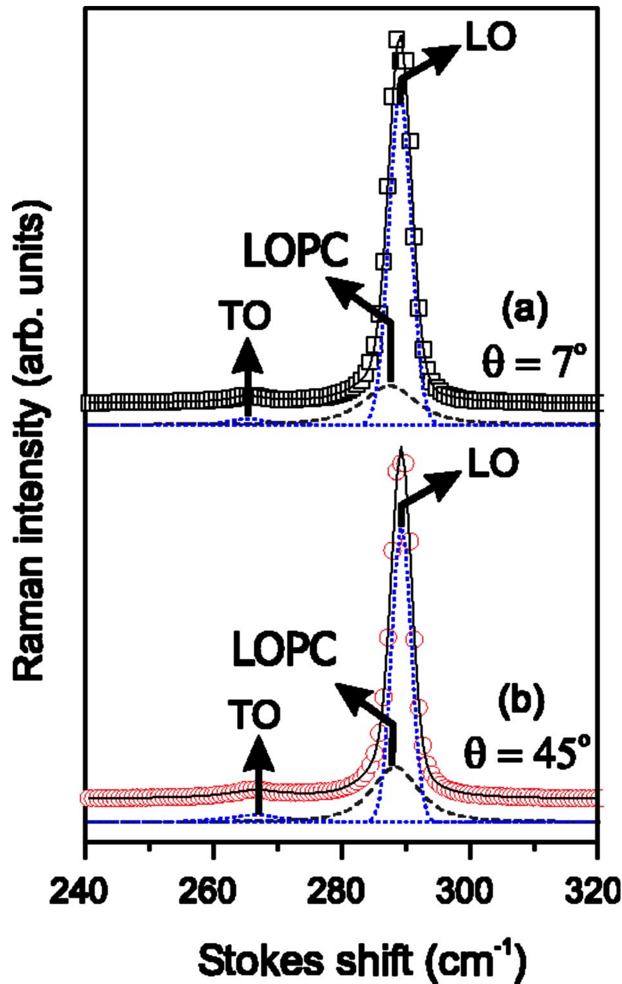

FIG. 5. Room temperature Raman spectra of As^+ implanted GaAs:Zn at 170 keV with ion beam oriented at 7° (a) and 45° (b) with respect to the surface normal.

that this type of defect affects the LOPC mechanism by modifying the local electron gas density.

Finally, in Figs. 3(b), 4(b), and 5(b) the LOPC modes are observed at 289, 287, and 289 cm^{-1}, whereas they appear at 285, 284, and 288 cm^{-1} in Figs. 3(a), 4(a), and 5(a), respectively. According to Ref. 11, such a spectral shift reveals higher carrier mobility in GaAs:Zn samples implanted at $\theta = 45°$. In agreement with the previous analysis, this result is attributed to lower crystal damage in the Raman probed volume, associated with nuclear cross-section lowering and ion channeling effects.[21]

TABLE I. Depletion layer depths deduced from the measured I_{LO}/I_{LOPC} areas ratios in ion implanted GaAs:Zn with tilt angles set to 7° and 45°, and projected range of implanted ion calculated using SRIM 2003 simulations.

Implantation		θ=7°		θ=45°	
Ion	Energy (keV)	d (nm)	R_p (nm)	d (nm)	R_p (nm)
P	40	44	37	28	30
As	90	40	39	21	29
	170	74	69	44	52

IV. CONCLUSION

Raman experiments carried out in the 240–320 cm^{-1} spectral range were used to investigate the defects generated by As outgassing in vacuum thermal annealed p-type GaAs:Zn between 250 and 450 °C. We have shown that the measurements of depletion layer depths agree with the expected changes of local free carrier density resulting from As atom displacements and desorption during RVTA.

We have also studied the crystal disorder associated with P^+ and As^+ implantations performed at different ion beam energies and tilt angles in $p = 7 \times 10^{18}$ cm^{-3} GaAs:Zn. The spectral signature of LO phonon and LOPC mode have allowed us to probe the damaged layers located up to 90 nm within the substrate. Our results make the Raman technique a simple and accurate technique to measure the range of defects induced by nuclear collisions during low-energy ion implantation.

ACKNOWLEDGMENT

The authors acknowledge financial support from NanoQuébec for this work.

[1] J. Wagner, M. Peter, K. Winkler, and K. H. Bachem, J. Appl. Phys. **83**, 4299 (1998).
[2] A. Saher Helmy, A. C. Bryce, C. N. Ironside, J. S. Aichison, and J. H. Marsh, Appl. Phys. Lett. **74**, 3978 (1999).
[3] K. Mizoguchi, S. Nakashima, Y. Sugiura, and H. Harima, J. Appl. Phys. **85**, 6758 (1999).
[4] F. Frost, G. Lippold, A. Schindler, and F. Bigl, J. Appl. Phys. **85**, 8378 (1999).
[5] R. Ashokan, K. P. Jain, H. S. Mavi, and M. Balkanski, J. Appl. Phys. **60**, 1985 (1986).
[6] K. Santhakumar, P. Jayavel, R. Kesavamoorthy, P. Magudapathy, K. G. M. Nair, and V. Ravinchandran, Nucl. Instrum. Methods Phys. Res. B **194**, 451 (2002).
[7] M. Seon, M. Holtz, W. M. Duncan, and T. S. Kim, J. Appl. Phys. **85**, 7224 (1999).
[8] T. Kamijoh, A. Hashimoto, H. Takano, and M. Sakuta, J. Appl. Phys. **59**, 2382 (1986).
[9] A. Mlayah, R. Carles, G. Landa, E. Bedel, and A. Muñoz-Yagüe, J. Appl. Phys. **69**, 4064 (1991).
[10] R. Fukasawa and S. Perkowitz, Phys. Rev. B **50**, 14119 (1994).
[11] G. Irmer, M. Wentzel, and J. Monecke, Phys. Rev. B **56**, 9524 (1997).
[12] A. Guillén-Cervantes, Z. Rivera-Alvarez, M. López-López, E. López-Luna, and I. Hernàndez-Calderón, Thin Solid Films **373**, 159 (2000).
[13] F. Proix, A. Akremi, and Z. T. Zhong, J. Phys. C **16**, 5449 (1983).
[14] J. F. Ziegler, J. P. Biersack, and U. Littmark, *The Stopping and Ion Range of Ions in Matter* (Pergamon, New York, 1985).
[15] E. Wendler, B. Breeger, C. Schubert, and W. Wesch, Nucl. Instrum. Methods Phys. Res. B **147**, 155 (1999).
[16] D. E. Aspnes and A. A. Studna, Phys. Rev. B **27**, 985 (1983).
[17] J. S. Blakemore, J. Appl. Phys. **53**, R123 (1982).
[18] D. Olego and M. Cardona, Phys. Rev. B **24**, 7217 (1981).
[19] T. E. Haynes, W. K. Chu, T. L. Aselage, and S. T. Picraux, J. Appl. Phys. **63**, 1168 (1988).
[20] C. Trallero-Giner, A. Cantarero, M. Cardona, and M. Mora, Phys. Rev. B **45**, 6601 (1992).
[21] P. D. Townsend, J. C. Kelly, and N. E. W. Hartley, *Ion Implantation, Sputtering and their Applications* (Academic Press, London, 1976), p. 45.
[22] Y. Kato, T. Shimada, Y. Shiraki, and K. F. Komatsubara, J. Appl. Phys. **45**, 1044 (1974).

Downloaded 20 Dec 2006 to 132.204.95.70. Redistribution subject to AIP license or copyright, see http://jap.aip.org/jap/copyright.jsp